Quaternary International 437 (2017) 98–106

Contents lists available at ScienceDirect

Quaternary International

journal homepage: www.elsevier.com/locate/quaint

Geochemical transect through a travertine mount: A detailed record of CO_2-enriched fluid leakage from Late Pleistocene to present-day – Little Grand Wash fault (Utah, USA)

Emanuelle Frery [a, *], Jean-Pierre Gratier [b, c], Nadine Ellouz-Zimmerman [d], Pierre Deschamps [e], Dominique Blamart [f], Bruno Hamelin [e], Rudy Swennen [g]

[a] CSIRO, Kensington, WA, USA
[b] ISTerre, Université Grenoble Alpes, 38041, Grenoble, France
[c] ISTerre, CNRS, 38041, Grenoble, France
[d] IFPEN, Rueil-Malmaison, France
[e] Aix-Marseille University, CNRS-IRD, CEREGE UM34, Europole Mediterraneen de l Arbois, BP80, 13545, Aix-en-Provence, France
[f] LSCE, Gif sur Yvette, France
[g] KU Leuven, Celestijnenlaan 200E, 3001, Heverlee, Belgium

ARTICLE INFO

Article history:
Available online 5 October 2016

Keywords:
Travertine
CO_2-enriched fluids
Leakage
U/Th dating
Oxygen and carbon stable isotopes
Vein growth rate

ABSTRACT

Active and fossil endogenic travertine mounts scattered along the Little Grand Wash fault are studied as records of Quaternary CO_2-enriched fluid leakage. This study focusses on a particular area where a fossil mount formed in a near-surface setting by successive circulation/sealing episodes from Late Pleistocene to Mid-Holocene and where a modern surface travertine is still being formed by a CO_2-enriched fluid source. The fossil mount is composed of horizontal and vertical veins whereby the vertical veins recorded numerous cycles of circulation/sealing/dissolution events and were used as conduits for the CO_2-enriched fluid circulation from the depth to the surface or along sub-horizontal fractures where successive precipitation events are recorded. The modern travertine is being built at the surface by successive eruption of Crystal Geyser, an anthropic geyser active since the 1930's.

$\delta^{13}C$ and $\delta^{18}O$ signatures and U/Th datings, ranging from 11.5 ky till present-day allows calibrating in detail the CO_2 enriched fluid leakage along a single fault segment and in a post glacial context, as last glaciations in the study area took place 15 ky ago. The dataset shows a high decrease of the oxygen stable isotope values till about 6 ky, then the variations reflect a constant range until present-day. This tends to restrain the period of local increase of the meteoric water input in the aquifer that is sourcing the CO_2-enriched water.

The fossil travertine represents a 7 ky-long record of CO_2 leakage above a natural reservoir, from Late Pleistocene to Mid-Holocene. The flux of CO_2 leakage through time and the total escaping volume have been computed and appears to be low in comparison with an anthropogenic leak provoked, for instance, by a non-sealed well.

1. Introduction

Endogenic travertines are records of paleoclimatic and paleotectonic events (Altunel and Hancock, 1993; Hancock et al., 1999; Faccenna et al., 2008; Brogi et al., 2010; Capezzuoli et al., 2010; De Filippis et al., 2011; Gratier et al., 2012; Priewisch et al., 2014; Ricketts et al., 2014; Frery et al., 2015). Travertines are calcium carbonate agglomerates known to be built under near ambient conditions in continental areas (Pentecost, 2005; Capezzuoli et al., 2014). Endogenic is use to define the origin of the CO_2-enriched fluids sourcing the agglomerate formation. Endogenic travertines are usually built along fault systems, where deep CO_2 and/or hot water are escaping from the depth to the surface (Janssen et al., 1999; Glover and Robertson, 2003; Crossey et al., 2006, 2009). Little Grand Wash present-day active travertine called Crystal Geyser is formed by cold water (~17 °C) with a heavy carbon isotope composition (>4‰, Kampman et al., 2009). The $\delta^{13}C$ and $\delta^{18}O$

* Corresponding author.
E-mail address: emanuelle.frery@csiro.au (E. Frery).

http://dx.doi.org/10.1016/j.quaint.2016.09.035
1040-6182/

signature of Green River fossil travertine mounts also demonstrate an endogenic origin of the fluids (Heath, 2004; Dockrill and Shipton, 2010). U/Th dating of these mounts calcium carbonate precipitations range from 400 ky to present-day (Burnside, 2010).

Such endogenic travertines located along Little Grand Wash and Salt Wash faults have been demonstrated to be formed episodically (Shipton et al., 2004; Dockrill, 2005; Burnside, 2010; Dockrill and Shipton, 2010; Kampman et al., 2012; Burnside et al., 2013; Frery et al., 2015). Kampman et al. (2013) showed that the CO_2 pulses can be related to glacial cycles.

In this contribution a detailed study of $\delta^{13}C$- and $\delta^{18}O$-signatures recorded along a travertine mount section is presented. U/Th dating and a part of the stable isotope measurements along this profile have been published in Frery et al. (2015) in order to build a conceptual model of episodic fluid circulation along an active fault. The record lasts from Late Pleistocene to present-day, providing a unique detailed record of this period of time that deserves to be closely analysed regarding i) the structure of the dated travertine veins; ii) the significance of the data regarding the Quaternary glaciation episodes on the Northwest part of the Colorado Plateau as well as iii) the calibration of CO_2 leakage during this period of time.

Results from more than 300 stable isotope analyses of the carbonate veins forming the travertine are analysed through time, based on 14 U/Th datings. Stable isotope measurements are shown for the whole dated period, from the thin section scale to the outcrop scale and on present-day active travertine forming close to the studied outcrop. Vertical and horizontal veins are studied regarding their petrography and their isotopic signature evolution through time. The results are then discussed in the perspective of the Late Holocene post-glacial cycle in the region and as potential proxy to calibrate the CO_2 paleo-leaky volumes along a particular segment of the fault during this period of time.

2. Location and sampling

The study focused on the so-called T1 fossil travertine mount, which is located in the footwall of a normal fault called Little Grand Wash (Fig. 1A and B). The mount is partially eroded. An accurate chronology has been obtained through 14 radiometric datings (U/Th) of 9 travertine veins sampled along a 10 m-thick profile (Fig. 1C). All samples were cleaned using a chemical pre-treatment to remove possible contamination. $^{234}U/^{230}Th$ ages were then measured with a TIMS mass spectrometer (CEREGE-Aix en Provence). The accuracy of the datings (from 11.469 to 4.559 ky) ranges from 27 to 9 years.

362 calcium carbonate powders (~1 mg each) were then collected using a dental drill on polished sections of 5 dated veins and 6 undated veins. These analyses were performed with an optima micromass spectrometer (LSCE, Gif sur Yvette, France). The accuracy on the measurements is ±0.04‰ and ±0.06‰ respectively for $\delta^{13}C$ and $\delta^{18}O$. The results are reported relative to

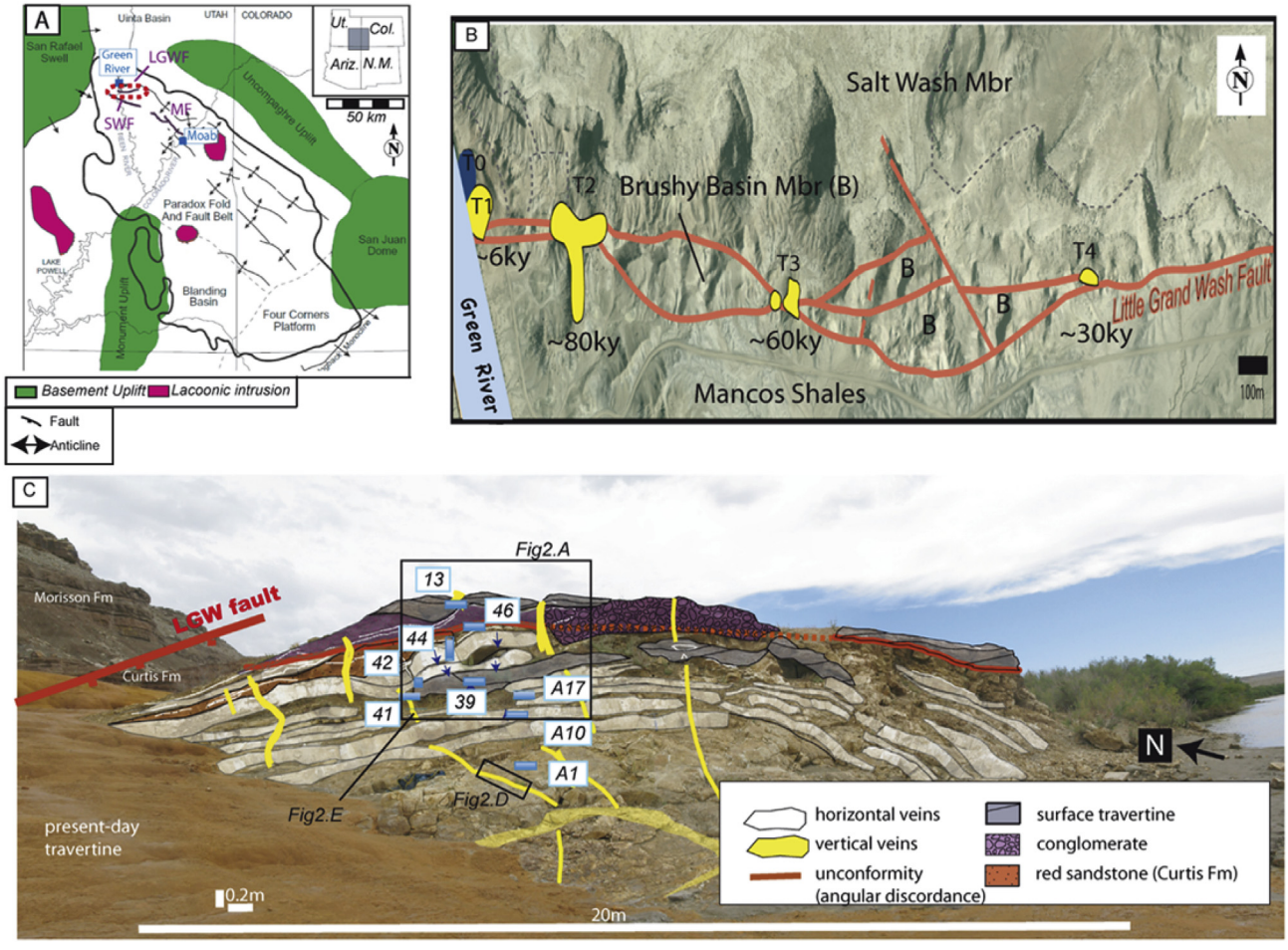

Fig. 1. Geological setting and sampling: (A) Location of the Little Grand Wash and Salt Wash faults within the Colorado Plateau. (B) Simplified geological map of Little Grand Wash fault. (C) Picture of the studied travertine mount and location of the sampling (modified from Condon, 1997; Dockrill, 2005 and Frery et al., 2015).

V-PDB and are given in the classical delta notation (Coplen et al., 1983).

Calcium carbonate powders were also sampled from thin sections for $\delta^{13}C$ and $\delta^{18}O$ analyses at the Friedrich-Alexander-University (Germany). Carbonate powders were reacted with 100% phosphoric acid at 75 °C using a Kiel III carbonate preparation line, connected online to a ThermoFinnigan 252 masspectrometer. All values were reported in permil relative to V-PDB by assigning a $\delta^{13}C$ value of +1.95‰ and a $\delta^{18}O$ value of −2.20‰ to NBS19. Reproducibility was checked by replicate analyses of laboratory standards and is better than 0.04‰.

Additional $\delta^{13}C$ and $\delta^{18}O$ analyses from the active Crystal Geyser travertine (location see Fig. 1) were acquired using the same technique and added to the dataset in order to get a range of current $\delta^{13}C$ and $\delta^{18}O$ values. Note that the CO_2-enriched water supplying the active travertine relates to the Glen Ruby #1, an oil well drilled in 1936 that was not sealed after been exploited for a few years. Thus the samples coming from this active travertine cannot be older than 80 years.

3. Results

3.1. Field observations

The fossil travertine mount reveals a complex internal structure, composed of calcium carbonate veins capped by conglomerates, i.e. pieces of the Curtis Formation outcropping in the hanging wall of the fault and a highly altered surface travertine (Fig. 1C).

Two main kinds of calcium carbonate veins can be distinguished thanks to their different orientation and internal structure, e.g. horizontal and vertical veins. The horizontal or sub horizontal veins (Fig. 2A–D) are characterized by their homogenous white colour and their subhorizontal parallel thin layering, parallel to the vein orientation. The vein growth direction is most of the time oriented from top to bottom and they are formed by calcium carbonate. The vein thickness is variable, from few centimetres to ten of centimetre thick.

The observed vertical veins (Fig. 2D, E, G) are formed by a series of calcium carbonate precipitation as well as other constituents such as micrite. “They are characterized by primary parallel

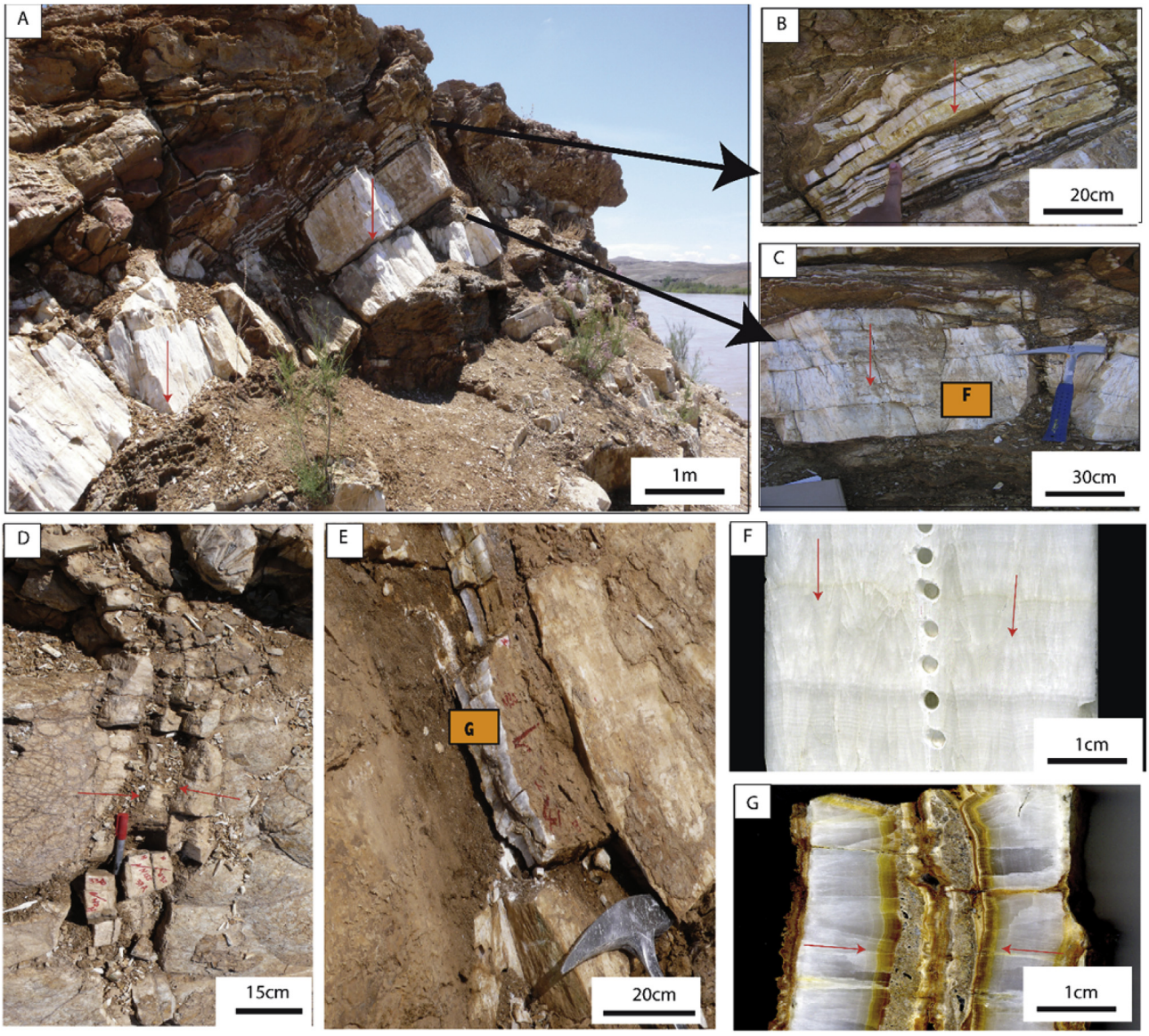

Fig. 2. Field observations along the fossil travertine mount outcrop (Fig. 1C). Note the difference between the horizontal veins (A, B, C and F) and the vertical veins (D, E and G). Growth direction illustrated by the red arrows. (For interpretation of the references to colour in this figure legend, the reader is referred to the web version of this article.)

precipitations, growing from the edges to the centre of the veines. Other events, such as micritisation, are also recorded, erasing this primary orientation."

3.2. $\delta^{13}C$ and $\delta^{18}O$ signature evolution from Late Pleistocene to present-day

$\delta^{13}C$ and $\delta^{18}O$ signatures of the carbonate veins sampled along the T1 profile and Crystal Geyser travertine mount are plotted in function of the recorded precipitation age obtained by U/Th dating of the travertine veins in Fig. 3. From Late Pleistocene till present-day, a general trend of both stable isotope values decreasing with time is observed (Fig. 3). The values can roughly be clustered into two groups. Group I values were deposited between 12 and 6 ky. It is characterized by $\delta^{18}O$ values decreasing from −11.5 to −13.5‰ and $\delta^{13}C$ from +5.5 to +5‰. The decrease of both isotopic signatures through time is apparent and both $\delta^{13}C$ and $\delta^{18}O$ variations are closely correlated. Group II datings range from 6 ky till present-day. $\delta^{18}O$ and $\delta^{13}C$ values are characterized by a rather constant variation range, respectively in the range −13.5 and −12.6‰ and +4.4 and +5‰. The dataset is more scattered and the correlation between the two isotopic signatures is less obvious than in the case of group I.

Both nature and origin of the CO_2-enriched fluids are quite stable through the recorded precipitation occurrences, as attested by the narrow range of variation of all the recorded isotopic values

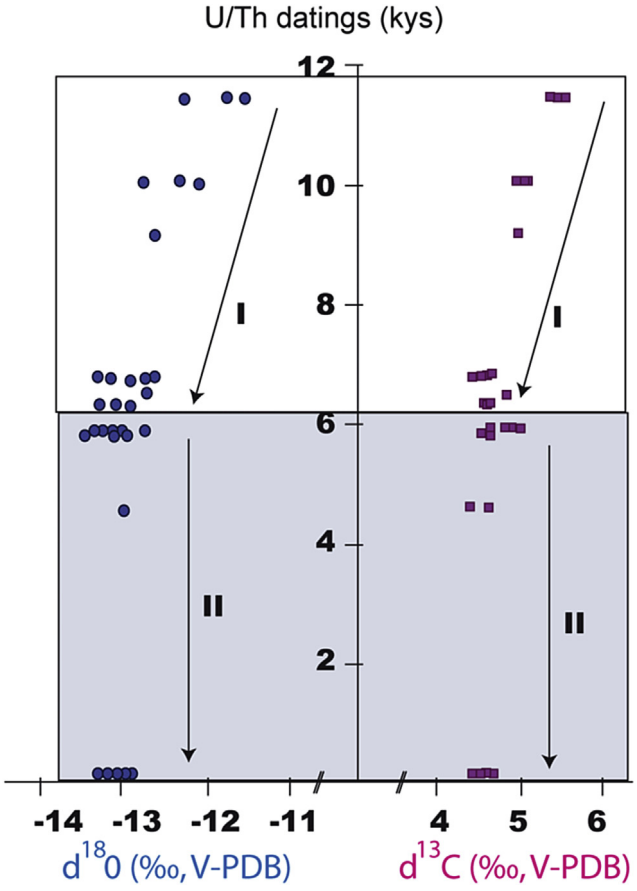

Fig. 3. Evolution of $\delta^{13}C$ and δ^{18O} signature (‰,V-PDB) in function of U/Th dating from Late Pleistocene till present-day, data coming from travertine T1 and present day Crystal Geyser travertine. Two groups of different signature I and II are found. Group I: $\delta^{13}C$ and δ^{18O} values decrease with time, Group II: $\delta^{13}C$ and δ^{18O} values are more or less stabilized.

(Fig. 3), from Late Pleistocene till present-day. However, a gap in the record appears between the youngest dated vein (4.559 ± 0.023 ky) of the fossil travertine T1 and the active travertine built by Crystal Geyser source. The youngest dated vein is located close by the top of the outcrop, only capped by altered layered surface travertine, consisting of material difficult to precisely date.

3.3. Successive precipitation events recorded in studied vertical veins

Several vertical veins have been sampled and studied at thin-section scale. These veins reflect numerous precipitation events, cross-cutting each other. For instance, at least 9 precipitation events can be sorted within a same vertical vein, as illustrated in detail in Fig. 4. The nature of the different types of mineralization, such as elongated thin aragonite or euhedral calcite crystals, indicate different mineralization processes and cycles of precipitation. The range in $\delta^{18}O$ and $\delta^{13}C$ variations between the different events recorded (Fig. 4C) is narrow, less than 1‰ for both isotopes. Based on this observation it is not unlikely that even if several cementation increments are observed, their isotopic signatures reflecting the CO_2-enriched fluid nature and origin, remain relatively similar. Detailed analysis of vertical vein systems showed a succession of precipitation events. Vertical veins can record several events of CO_2-enriched fluid precipitation, dissolution and new precipitation events and thus does not necessarily represent an archive of the precipitation that occurred at a given time.

3.4. Continuous dated geochemical records from studied horizontal veins

Studied horizontal veins are formed by discrete travertine successions providing a better record of the successive precipitations between two dated samples. The thickest carbonate veins of the outcrop (veins 42 and 44 located in Fig. 1) were studied in detail (Fig. 5) with a punctual isotopic analysis each 2–5 mm and a U/Th dating every 100–150 mm. Such horizontal travertine veins grow from top to bottom and thus lifted the rocks above them. This is explained by the effect of crystallization force (Gratier et al., 2012).

From the U/Th dating, a linear vein growth rate has been estimated from 0.08 to 0.71 mm/yr. However, the growth rate is variable along the vein trajectory and its value is highly dependent on the interval of time considered to make the interpolation. Nevertheless, a continuous rising of the growth rate is noticeable during the entire period of time recorded in both veins, from 11.469 to 5.851 ky (Fig. 5).

The oldest vein (44), formed in the period 11.469 ± 0.015 till to 9.175 ± 0.014 ky, shows two patterns with regard to its stable isotope signature, e.g.: i) for the period between 11.469 ± 0.015 till 10.053 ± 0.012 ky, where both $\delta^{13}C$ and $\delta^{18}O$ decrease and ii) from 10.053 ± 0.012 till 9.175 ± 0.014 ky, the correlation between the two isotope ratios is less obvious and the average value remains rather constant. The other vein (42), which dates from 6.830 ± 0.014 till 5.851 ± 0.010 ky, does not reflect any correlation between $\delta^{18}O$ and $\delta^{13}C$ and the average values remain rather constant.

Two millennial evolutionary trends were thus observed: 1) decrease and close correlation of stable isotope ratios or 2) linear behaviour with time and without a close correlation in $\delta^{18}O$ and $\delta^{13}C$ ratio variations. In parallel, a near constant growth rate (0.1–0.2 mm/y) is observed from 11.5 to 6 ky, then an increase of this growth rate up to 0.7 mm/y since 6 ky.

Both horizontal veins are continuously laminated, with laminations occurring parallel to the vein opening plane.

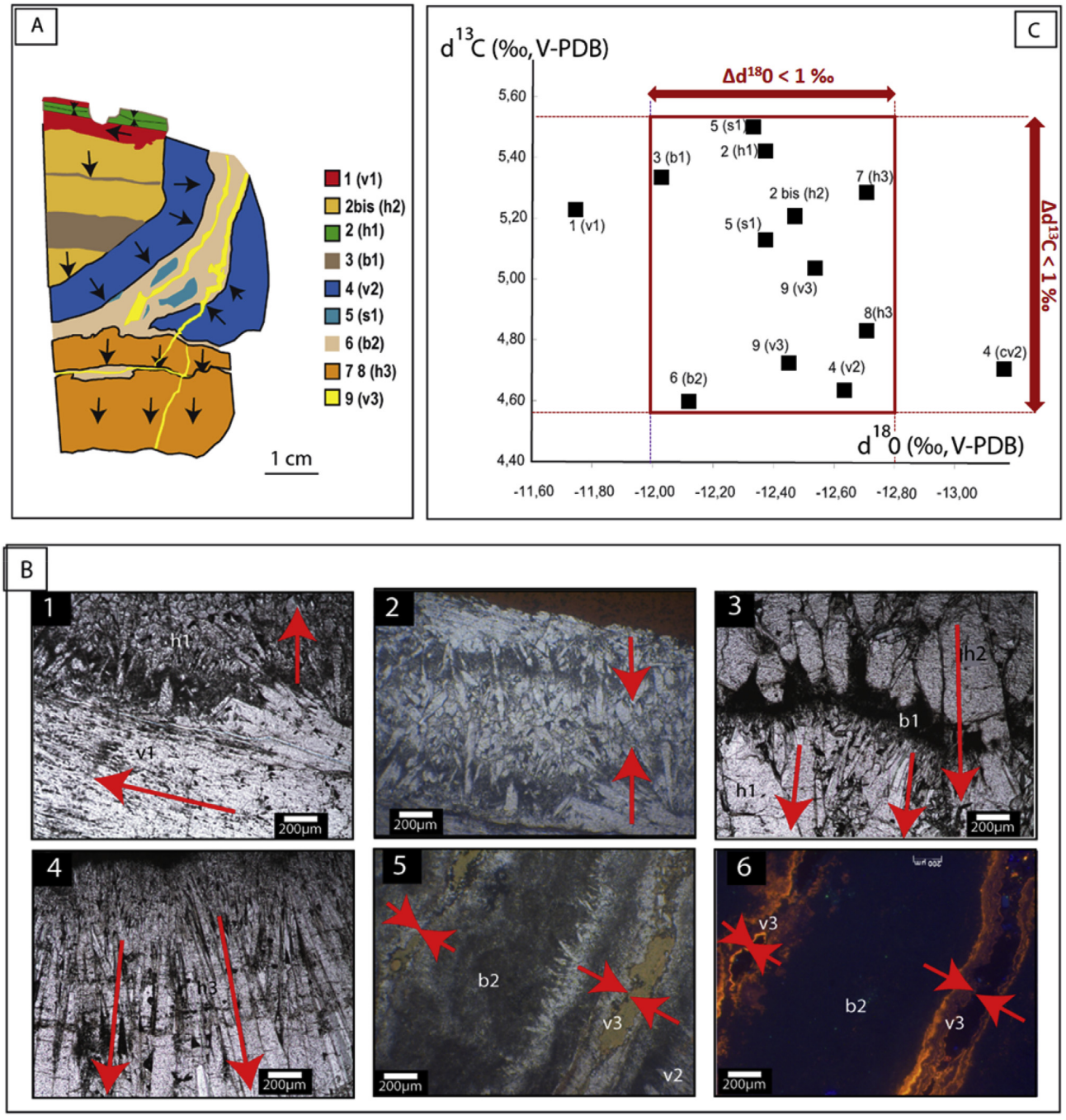

Fig. 4. Details of different vein generations: example of a thin section from travertine T1, little Grand Wash fault (localized Fig. 1C). A. Records of mineralization episodes at the thin-section scale. The colours reflect the different diagenetic events. The nature of these events is specified in parentheses (v vertical carbonate vein; h horizontal carbonate vein; s: sandstone; b: micrites). The arrows give the mineral growth direction and senses of each event. The order of apparition of each event is in the legend: 1 for the oldest and 9 for the youngest. Detailed of the sealing relative chronology may be summarized as follows: a) The vertical fibrous vein v1 had been sealed by elongated thin aragonite phases (picture B 1). This vein is almost fully erased by the other mineralization stages. b) v1 is crossed by a horizontal thin vein with centripetal growth (h1) filled with a euhedral-calcite mineralization with an open space in the middle (picture B 2). c) Then, there is another horizontal vein (h2) of aragonite including micritic laminations (b1) and altered aragonite crystals (picture B 3). d) Other centripetal growth nearly vertical veins with subhorizontal mineralization (v2) crosscut the system h1/b1. At the middle, micrite (b2) and sand infill (s1) are present. This sandstone may originate from the Green River that is located near the outcrop. e) This is cut by other later horizontal veins (h3). These veins are composed of compact aragonite with top-to-bottom growth direction (4). f) The last vertical veins (v3) cross-cut the entire thin-section. The associated precipitations consist of euhedral centripetal growth calcium carbonate with an empty space in the middle (picture B 5). The cathodoluminescence study shows an orange colour, reflecting a difference in composition between this vein and the other phases which are non-luminescent (picture B 6). B. Pictures of the different mineralisation events observed on the thin-section localised on A – the mineral growth direction is indicated with red arrows. 1. A piece of vertical vein v1 with associated horizontal aragonite fibres is crossed by a horizontal vein h1 with vertical fibres – 2. Thin horizontal vein h1 with centripetal growth characteristics. – 3. Detail of the horizontal veins h2 top to bottom growth: altered aragonite minerals with micritic laminations b1. – 4. Compact aragonite phases in the horizontal top to bottom growth vein h3. – 5 & 6. Respectively natural light and cathodoluminescence image of the last mineralization event with the centripetal growth of vertical thin vein v3 crossing the micritic event b2. The veins v3 are clearly orange. C. $\delta^{13}C$ and $\delta^{18}O$ (‰, V-PDB) from the veins observed on the thin section (A). The nature of each phase is specified in brackets (v vertical carbonate vein; h horizontal carbonate vein; s: sandstone; b: micrites). The main part of the samples, excepted 1 (v1) and 4 (cv2), have similar $\delta^{13}C$ and $\delta^{18}O$ signature, with a variation range, $\Delta\ \delta^{13}C$ and $\delta^{18}O$, inferior to 1‰. (For interpretation of the references to colour in this figure legend, the reader is referred to the web version of this article.)

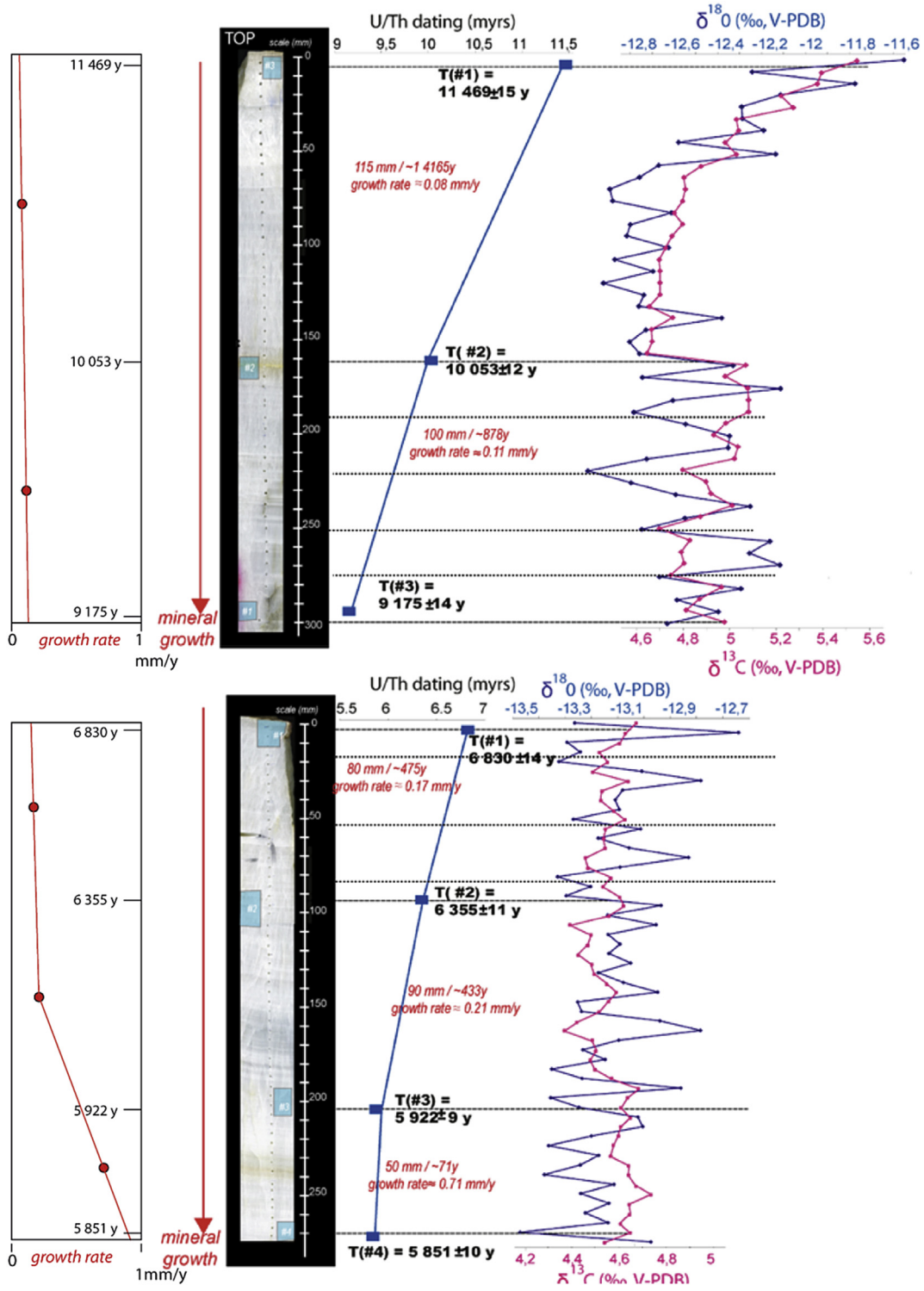

Fig. 5. Evolution of the stable isotopes signature (‰ V-PDB) and mineral growth rate in function of U/Th dating illustrated by two carbonate veins named 42 and 44 located in Fig. 1C. The growth rate is near constant from 11,5 to 6 ky then increase since 6 ky. In parallel, one can see two millennial geochemical evolutionary trends: 1) decrease and strong correlation of $\delta^{13}C$ and $\delta^{18}O$ or 2) linear behaviour with time and a possible opposed $\delta^{18}O$ and $\delta^{13}C$ ratio evolution.

4. Discussion

4.1. A detailed geochemical record of a post glacial interval

Green River fault leakage has been studied over the past 400,000 years on 40 separated travertine mounds by Kampman et al. (2012). This present study completes this regional work with a detailed dataset focussed on the record of Late Pleistocene to present-day CO_2-enriched fluid flow. The studied T1 travertine mount records carbonate precipitations from 11.469 ± 0.015 ky ago up to 4.559 ± 0.023 ky ago, thus archiving up to 7 ky of precipitation history at this location.

During this period, travertine precipitation was not constant through time: vein sizes are variable and some periods of time are marked by a high frequency of sealing whereas other periods are marked by a lack of record (Figs. 2 and 5).

From 11.469 ± 0.015 till 10.053 ± 0.012 ky, $\delta^{13}C$ and $\delta^{18}O$ values decrease with a high covariant variation. This covariant change observed at the vein scale possibly indicates kinetically-driven vein precipitation (Kele et al., 2011; Kampman et al., 2013). Kampman et al. (2012) demonstrated a causal relationship between CO_2-pulsing and vein opening by isotopic analyses (C, O, Sr ratio and Ba/Ca and Sr/Ca elemental ratio). The opening of the veins is linked with a pulse of CO_2 in the system followed by a degassing step contemporaneous to the vein growth. The pulse of CO_2 is marked by a decrease in $\delta^{13}C$-values and the degassing by a rise in $\delta^{13}C$. Our data tends to record a pulse of CO_2 in the system. This variation in $\delta^{13}C$ and $\delta^{18}O$ correlation is due to isotope fractionation between C present as CO_2 (aq) and HCO_3^- in the spring waters and carbon in $CaCO_3$. The extreme enrichment in ^{13}C in the veins is then a result of Rayleigh fractionation during degassing of the fluid (Kampman et al., 2012). The vein samples enriched in heavier $\delta^{13}C$ compared to $\delta^{13}C$ composition of the present-day Crystal Geyser water (<1.5‰ VPDB, Heath, 2004) may be due to rapid CO_2 degassing (Fouke et al., 2000; Fouke, 2011).

This study recorded $\delta^{18}O$ highly decrease in the older samples from 11.5 to 10.5 ky and then keep clearly decreasing up to 6 ky. This result aligns with the Green River travertine mounts evolution trend (Kampman et al., 2013) that reflects a mean general decrease of around 1‰ for the last 15 ky. This detailed U/Th, $\delta^{18}O$, $\delta^{13}C$ record suggests that the main decrease period observed in $\delta^{18}O$ signature is taking place at the end of the Pleistocene, in a short period of time that ended less than 9 ky after the last local glaciation that took place 15 ky ago (Marchetti et al., 2011). Then, from 6 ky, the $\delta^{18}O$ values remain quite constant until present-day. $\delta^{18}O$ recorded in the travertine is function of the water temperature and $\delta^{18}O$ as well as other environmental factors, such as evaporation (Andrews, 2006). Present-day chemical and isotopic analyses of Crystal Geyser bubbling water suggested a mix origin: meteoritic water mixed with groundwater from the Jurassic Navajo regional aquifer with the input of deep CO2 from a paleozoic aquifer (Kampman et al., 2009). The water $\delta^{18}O$ values are quite constant, with a smooth 0.3‰ oscillation (from −14.4 to −14.1‰ SMOW, Heath, 2004). Study of other active bubbling springs along the Little Grand Wash fault and Salt Wash fault showed a similar fluid origin with a $\delta^{18}O$ values are quite constant, with less that 1‰ variation that could be directly explained by the water temperature range, 16.7 to 17.7 °C, from one spring to another (Heath et al., 2009).

The Quaternary $\delta^{18}O$ values decrease in Green River area had been interpreted as a potential post glacial increase of meteoric water in the system (Kampman et al., 2012). This study dataset shows that, in this hypothesis, the post-glacial increase of meteoritic water in the system is rapid until 6 ky and then do not evolve considerably until present-day. The immediate post-glacial period (11.5 till 6 ky) is also marked by a slow grow rate (0.08 mm/y) of the vein (Fig. 5). Following this period, the vein grow rate rises up to 0.71 mm/y at least between 6,1 and 5,8 ky (no data are available later) and the $\delta^{13}C$ and $\delta^{18}O$ variations stay constant, from 6 ky till present-day (Fig. 3).

4.2. CO_2 leakage from Late Pleistocene to Mid Holocene

The total volume of CO_2 leakage at the surface can be estimated from the volume of calcium carbonate precipitated in the travertines.

At the Crystal Geyser outlet, based on hydrologic mass balance modelling of the present−day CO_2 water composition, some authors (Heath, 2004; Shipton et al., 2005) estimated the proportion of the total CO_2 flux accounting for travertine mount formation. They estimated that the volume of CO_2 leakage recorded in the calcium carbonate precipitations represents between 6.6% (Heath, 2004) and 10% (Shipton et al., 2005) of the total dissolved CO_2 in the water sample, which is only a minor part of the total leakage. Based on these estimations, a minimal value of the CO_2 leakage can be estimated from the T1 record, as the CO_2 escaping as a free phase is not taking into account in the chemical models based on the water sampling and that the travertine outcrop has been partially eroded.

In the case of the T1 fossil travertine mount studied here (Fig. 1C), the total mass of precipitated CO_2 recorded in the outcrop over time was calculated considering the calcium carbonate precipitation equation (Eq. (1)):

$$m_{CO_2}^{precipitated} = \rho_{CaCO_3} \cdot V_{CaCO_3} \frac{M_{CO_2}}{M_{CaCO_3}} \quad (1)$$

The molar mass ratio of carbon dioxide and calcium carbonate and the volume density of the calcium carbonate are considered as constant parameters:

$$\frac{M_{CO_2}}{M_{CaCO_3}} = \frac{44 g.mol^{-1}}{100,1 g.mol^{-1}}$$

$$\rho_{CaCO_3} = 2,7.10^3\ kg.m^{-3}$$

Eq. (1) can therefore be simplified so that the mass of precipitated CO_2 is a direct function of the volume of calcium carbonate precipitated:

$$m_{CO_2}^{precipitated} = 119 \cdot V_{CaCO_3} \quad (2)$$

In order to calculate the volume of calcium carbonate (V_{CaCO_3}) a 5 m long rectangular section along the travertine with a 1 m^2 surface base was considered (Fig. 1C). The dated veins represent 45 ± 10% of the total block volume of the travertine mount T1. The veins are considered to be rectangular parallelepipeds with thicknesses as measured in the field and the initial surface area of the travertines being extrapolated to its initial value before erosion. This initial value has been extrapolated from present-day measurements of travertine T1 surface calculation, based on aerial photos (Dockrill, 2005) and our structural analysis. Details of the CO_2 volume and leakage flow computations are given in Table 1.

The total CO_2 leakage flow, inferred from the U/Th dated veins (Fig. 6), shows an interesting evolution through this studied period of time (11.5 ky till 4 ky): the temporal variation in CO_2 flow is episodic with 4 mean periods of fluid flow and vein sealing that last about half of the total period duration (Fig. 6). Consequently, even if the total mass of CO_2 emissions is difficult to determine, a new minimum value of CO_2 leakage in natural conditions is calibrated. The total natural CO_2 leakage flow inferred from the travertine mass is low, less than 0.9 tonnes per year. For comparison, the present-day monitoring of Crystal Geyser allow to calibrate a high seepage rate of 11.000 tonnes/year (Gouveia et al., 2005; Brogen et al., 2006). This

Table 1
Volume and flux of CO_2 leakage recorded in the travertine mound from Late Pleistocene to present-day. The total CO_2 volume is extrapolated from the travertine mount volume and two hypotheses on this fraction percentage of the total leaky CO_2: 6.6% and 10% (Heath, 2004; Shipton et al., 2005).

	Veins fraction (% ±5%)	Fraction of the travertine mount (% ±5%)	Veins thickness (mm ± 5%)	Mass CO_2 precipitated (T ± 30%)	Mass total of CO_2 leakage (T ± 30%)		Growth rate (mm/y ± 10%)	Leakage time-lapse (y ± 15%)	Flux of CO_2 leakage (T/ky ± 40%)	
					6.6%	10%			**6.6%**	**10%**
A1	15	6,8	203	48	730	482	0,1	2025	361	238
A10	15	6,8	203	48	730	482	0,1	2025	361	238
A17	15	6,8	203	48	730	482	0,1	2025	361	238
39	4	1,8	54	13	195	129	0,7	77	2524	1666
42	20	9,0	270	64	974	643	0,2–0,7	988	985	650
44	23	10,4	311	74	1120	739	0,08–0,1	2282	491	324
46	6	2,7	81	19	292	193	0,4	203	1442	952
41	1	0,5	50	0	3	2	0,7	71	38	25
13	1	0,5	80	0	4	3	0,7	114	38	25
Tot dated veins	100	45	1350	321	4868	3213	0,4	7285	668	441
Tot undated veins		15	600	143	2164	1428	0,4	7285	297	196
Tot travertine veins		60	1800	428	6491	4284	0,4	7285	891	588
Tot carbonate travertine		70	2100	500	7573	4998	0,4	7285	1039	686

geyser is indeed being sourced from an abandoned well that crosscuts the regional seal and that was not totally closed after its production. This CO_2 flux is 10.000 times greater than the flux computed from the travertine mount that was formed by a natural CO_2 leakage along the fault. This highlights the preponderant role of the episodic sealing of the fault that controls the fluid flow (Frery et al., 2015). For instance, considering natural flow (computed in this study), the release of the 11 million tons of CO_2 stored in the Sleipner field, in the North Sea (Hermanrud et al., 2009; Chadwick et al., 2011) would take more than 10 My, whereas it would take only 1000 years if an open hole drilled through the reservoir were allowed to leak permanently without being sealed.

5. Conclusion

The studied endogenic travertine, located in the footwall of Little Grand Wash Fault, along the NW part of the Colorado Plateau, recorded CO_2-enriched fluid leakage from Late Pleistocene till Mid Holocene. The detailed $\delta^{13}C$ and $\delta^{18}O$ dataset along T1 travertine mount profile represents a unique archive of the CO_2-enriched fluids evolution along a single segment of a fault. The record corresponds to a period of time following the last glacial event, which locally took place 15 ky ago.

Until 6 ky ago, the record is dominated by CO_2 pulses, rapid decrease of the $\delta^{18}O$ values and a low growth rate of the travertine veins. The decrease of the $\delta^{18}O$ values can indicate an increase of the meteoritic water concentration in the system (Kampman et al., 2012). Following that period, the $\delta^{18}O$ values tend to equilibrium and episodes of lower amplitude CO_2 pulses occurred in correlation with an increase in growth rate. These episodes can be linked with the fault tectonics as supported by the development of different vertical and horizontal veins. The vertical veins record several cycles of sealing/dissolution/sealing, acting as conduit for CO_2-enriched fluids input in the system as described in Frery et al. (2015) from the same outcrop. Note that this kind of episodic leakage through the fault is also well described in a tectonically

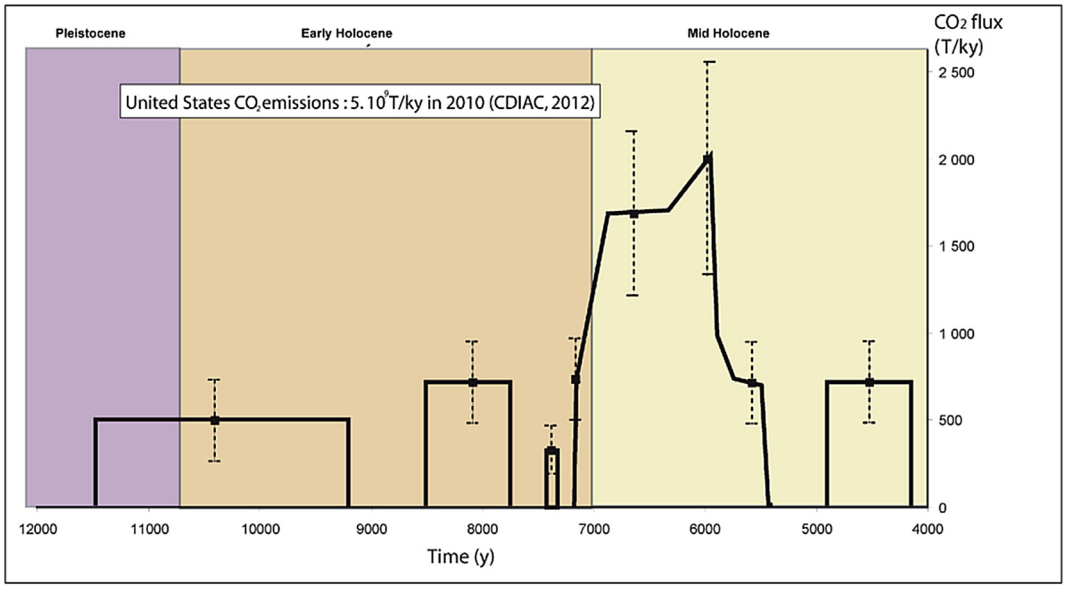

Fig. 6. Evolution of cumulative leaky CO_2 flux in function of time from the Late Pleistocene till the Mid Holocene, computed from U/Th dated aragonite veins of travertine T1, Little Grand Wash Fault. The flux has been computed from the volume estimation of each vein averaged over the vein thickness. The veins are located in Fig. 1C and the modelling results are shown Table 1.

active context from fissure ridge travertine mounts near Pamukkale (Turkey) (Brogi et al., 2014) where the vertical veins emplacement changed through time, migrating towards the fault hanging wall.

The travertine mount has also been used as a proxy to evaluate the rate of CO_2 leakage from Late Pleistocene to Mid Holocene. The total natural CO_2 leakage flow inferred from the travertine mass is low, less than 0.9 tonnes per year. A comparison with CO_2 leakage along an open hole near by the studied travertine mount that has been left open shows that anthropogenic CO_2 flux is 10.000 times greater than natural CO_2 leakage along the fault. This highlights the preponderant role of the sealing of the faults that controls the fluid flow. It illustrates that open holes seem to heal much more slowly than natural faults.

Acknowledgements

The authors would like to acknowledge Laura Crossey as well as an anonymous reviewer for their constructive comments that helped to improve this manuscript. We also would like to thanks Herman Nijs who made the thin sections, Prof. M. Joachimsky (University of Erlangen, Germany) for his support on the stable isotope measurement and IFPEN for the financial support.

Appendix A. Supplementary data

Supplementary data related to this article can be found at http://dx.doi.org/10.1016/j.quaint.2016.09.035.

References

Andrews, J.E., 2006. Paleoclimatic record from stable isotopes in riverine tufas: synthesis and review. Earth-Science Reviews 75, 85–104.
Altunel, E., Hancock, P.L., 1993. Morphology structural setting quaternary travertines pamukkale, Turkey. Geological Journal 28 (3), 335–346.
Brogen, K.T., Homann, S.G., Gouveia, F.J., Neher, L.A., 2006. Prototype near-field/Gis model for sequestrated-CO_2 risk characterization and management. In: Proceedings of the International symposium on site characterization for CO_2 Geological Storage, March 20th, 2006, Berkeley, CA.
Brogi, A., Capezzuoli, E., Aque, R., Branca, M., Voltaggio, M., 2010. Studying travertines for neotectonics investigations: Middle-Late Pleistocane syn-tectonic travertine deposition at Serre di Rapolano (Northern Apennines, Italy). International Journal of Earth Sciences 99 (6), 1383–1398.
Brogi, A., Capezzuoli, E., Cihat Alcicek, M., Gandin, A., 2014. Evolution of a fault-controlled fissure-ridge travertine deposit in the western Anatolia extensional province: the Cukurbag fissure-ridge (Pamukkale, Turkey). Journal of the Geological Society, London 171, 425–441.
Burnside, N.M., 2010. U-Th Dating of Travertine on the Colorado Plateau: Implications for the Leakage of Geologically Stored CO_2 (Ph.D. thesis). University of Glasgow, England, p. 290.
Burnside, N.M., Shipton, Z.K., Dockrill, B., Ellam, R.M., 2013. Man-made versus natural CO_2 leakage: a 400 ky. history of an analogue for engineered geological storage of CO_2. Geology 41 (4), 471–474.
Capezzuoli, E., Gandin, A., Sandrelli, F., 2010. Calcareous tufa as indicators of climatic variability: a case study from southern Tuscany (Italy). The Geological Society of London 336, 263–281.
Capezzuoli, E., Gandin, A., Pedley, M., 2014. Decoding tufa and travertine (fresh water carbonates) in the sedimentary record: the state of the art. Sedimentology 61, 1–21.
Chadwick, R.A., Noz, D., Arts, R., Eiken, O., 2011. Latest time-lapse seismic data from Sleipner yield new insights into CO_2 plume development. Energy Procedia 1 (1), 2103–2110.
Condon, S.M., 1997. Geology of the Pennsylvanian and Permian Cutler Group and Permian Kaibab Limestone in the Paradox Basin, Southeastern Utah and Southwestern Colorado. U.S.Geological Survey Bulletin 2000.
Coplen, T.B., Kendall, C., Hopple, J., 1983. Comparison of stable isotope reference samples. Nature 302, 236–238.
Crossey, L.J., Fischer, T.P., Patchett, P.J., Karlstrom, K.E., Hilton, D.R., Newell, D.L., Huntoon, J., Reynolds, A.C., De Leeuw, G.A.M., 2006. Dissected hydrologic system at the Grand Canyon: interaction between deeply derived fluids and plateau aquifer waters in modern springs and travertine. Geology 34 (1), 25–28.
Crossey, L.J., Karlstrom, K.E., Springer, A.E., Newell, D., Hilton, D.R., Fischer, T., 2009. Degassing of mantle-derived CO_2 and He from springs in the southern Colorado Plateau region—Neotectonic connections and implications for groundwater systems. Geological Society of America Bulletin 121 (7–8), 1034–1053.
De Filippis, L., Faccenna, C., Funiciello, R., Billi, A., Soligo, M., Rossetti, C., Tuccimei, P., 2011. The Lapis Tiburtinus travertine (Tivoli, Central Italy): its controversial tectonic vs paleoclimatic origin. Rendiconti Online Della Società Geologica Italiana 16, 15–16.
Dockrill, B., 2005. Understanding Leakage from a Fault-sealed CO_2 Reservoir in East-Central Utah: a Natural Analogue Applicable to CO_2 Storage (Ph.D. thesis). University of Dublin, Trinity College, p. 165.
Dockrill, B., Shipton, Z.K., 2010. Structural controls on leakage from a natural CO_2 geologic storage site: Central Utah, USA. Journal of Structural Geology 32 (11), 1768–1782.
Faccenna, C., Soligo, M., Billi, A., De Filippis, L., Funiciello, R., Rossetti, C., Tuccimei, P., 2008. Late Pleistocene depositional cycles of the Lapis Tiburtinus travertine (Tivoli, Central Italy): possible influence of climate and fault activity. Global and Planetary Change 63 (4), 299–308.
Fouke, B.W., Farmer, J.D., Des Marais, D.J., Pratt, L., Sturchio, N.C., Burns, P.C., Discipulo, M.K., 2000. Depositional facies and aqueous-solid geochemistry of travertine-depositing hot springs (Angel Terrace, Mammoth hot springs, Yellowstone National Park, USA). Journal of Sedimentary Research 70 (3), 565–585.
Fouke, B.W., 2011. Hot-spring systems Geobiology: abiotic and biotic influences on travertine formation at Mammoth hot spring, Yellowstone National Park, USA. Sedimentology 58 (1), 170–219.
Frery, E., Gratier, J.P., Ellouz-Zimmerman, N., Loiselet, C., Braun, J., Deschamps, P., Blamart, D., Hamelin, B., Swennen, R., 2015. Evolution of fault permeability during episodic fluid circulation: evidence for the effects of fluid-rock interactions from travertine studies (Utah-USA). Tectonophysics 651–652, 121–137. http://dx.doi.org/10.1016/j.tecto.2015.03.018.
Glover, C., Robertson, A.H.F., 2003. Origin of tufa (cool-water carbonate) and related terraces in the Antalya area, SW Turkey. Geological Journal 38 (3–4), 329–358.
Gouveia, F.J., Johnson, M.R., Leif, R.N., Friedman, S.L., 2005. Aerometric Measurement and Modeling of the Mass of CO_2 Emissions from Crystal Geyser, Utah. UCRL-TR-211870. Lawrence Livermore National Lab, Livermore, CA (US).
Gratier, J.-P., Frery, E., Deschamps, P., Røyne, A., Renard, F., Dysthe, D., Ellouz-Zimmerman, N., Hamelin, B., 2012. How travertine veins grow from top to bottom and lift the rocks above them: the effect of crystallization force. Geology 40, 1015–1018.
Hancock, P.L., Chalmers, R.M.L., Altunel, E., Cakir, Z., 1999. Travitonics: using travertines in active fault studies. Journal of Structural Geology 21 (8–9), 903–916.
Heath, J.E., 2004. Hydrogeochemical Characterization of Leaking Carbon Dioxide-charged Fault Zones in East-Central Utah. Master Thesis. Utah State University, Logan, Utah, p. 166.
Heath, J.E., Lachmar, T.E., Evans, J.P., Kolesar, P.T., Williams, A.P., 2009. Hydrogeochemical Characterization of Leaking, Carbon Dioxide-Charged Fault Zones in East-Central Utah, With Implications for Geologic Carbon Storage. Carbon Sequestration and Its Role in the Global Carbon Cycle, pp. 147–158.
Hermanrud, C., Andersen, T., Eiken, O., Hansen, H., Janbu, A., Lippard, J., Bolàs, H.N., Simmenes, T., Teige, G.M.G., Ostmo, S., 2009. Storage of CO_2 in saline aquifers-Lessons learned from 10 years of injection into the Utsira formation in the Sleipner area. Energy Procedia 1 (1).
Janssen, A., Swennen, R., Podoor, N., Keppens, E., 1999. Biological diagenetic influence recent fossil tufa deposits from Belgium. Sedimentary Geology 126 (1), 75–95.
Kampman, N., Bickle, M., Becker, J., Assayag, N., Chapman, H., 2009. Feldspar dissolution kinetics and Gibbs free energy dependence in a CO_2-enriched groundwater system, Green River, Utah. Earth and Planetary Science Letters 284 (3–4), 473–488.
Kampman, N., Burnside, N.M., Shipton, Z.K., Chapman, H.J., Nocholl, J.A., Ellam, R.M., Brickle, M.J., 2012. Pulses of carbon dioxide emissions from intracrustal faults following climatic warming. Nature Geoscience 5, 352–358.
Kampman, N., Bickle, M., Maskell, A., Chapman, H.J., Evans, J.P., Purser, G., Zhou, Z., Schaller, M.F., Gattacceca, J.C., Bertier, P., Chen, F., Turchyn, A.V., Assayag, N., Rochelle, C., Ballentine, C.J., Busch, A., 2013. Drilling and sampling a natural CO_2 reservoir: implications for fluid flow and CO_2-fluid-rock reactions during CO_2 migration through the overburden. Chemical Geology 369, 51–82.
Kele, S., Özkul, M., Gökgöz, A., Baykara, M.O., Alçiçek, M.C., Németh, T., 2011. Stable isotope geochemical study of Pamukkale travertines: new evidences of low-temperature non-equilibrium calcite-water fractionation. Sedimentary Geology 238, 191–212.
Marchetti, D.W., Harris, M.S., Bailey, C.M., Cerling, T.E., Bergman, S., 2011. Timing of glaciation and last glacial maximum paleoclimate estimates from the Fish Lake Plateau, Utah. Quaternary Research 75, 183–195.
Pentecost, A., 2005. Travertine. Springer-Verlag Berlin Heidelberg, p. 305.
Priewisch, A., Crossey, L.J., Karlstrom, K.E., Polyak, V.J., Asmerom, Y., Nereson, A., Ricketts, J.W., 2014. U-series geochronology of large-volume quaternary travertine deposits of the southeastern Colorado Plateau: evaluating episodicity and tectonic and paleohydrologic controls. Geosphere 10 (2), 401–423.
Ricketts, J.W., Karlstrom, K.E., Priewisch, A., Crossey, L.J., Polyak, V.J., Asmerom, Y., 2014. Quaternary extension in the Rio Grande rift at elevated strain rates recorded in travertine deposits, central New Mexico. Lithosphere 6 (1), 3–16.
Shipton, Z.K., Evans, J.P., Kirchner, D., Kolesar, P.T., Williams, A., Heath, J., 2004. Analysis of CO_2 Leakage through "low-permeability" Faults from Natural Reservoirs in the Colorado Plateau, Southern Utah, vol. 233, pp. 43–58. Geological Society, London, Special Publications.
Shipton, Z.K., Evans, J.P., Dockrill, B., Heath, J., Williams, A., Kirchner, D., Kolesar, P.T., 2005. Natural leaking CO_2-charged systems as analogs for failed geologic storage reservoirs. In: Thomas, D. (Ed.), Carbon Dioxide Capture for Storage in Deep Geologic Formations -Results from the CO_2 Capture Project, vol. 2. Elsevier Science, pp. 699–712.

Web site:

Carbon Dioxide Information Analysis Center:http://cdiac.ornl.gov/.